

## Phonon-Induced Spin-Spin Interactions in Diamond Nanostructures: Application to Spin Squeezing

S. D. Bennett,<sup>1</sup> N. Y. Yao,<sup>1</sup> J. Otterbach,<sup>1</sup> P. Zoller,<sup>2,3</sup> P. Rabl,<sup>4</sup> and M. D. Lukin<sup>1</sup>

<sup>1</sup>Physics Department, Harvard University, Cambridge, Massachusetts 02138, USA

<sup>2</sup>Institute for Quantum Optics and Quantum Information, Austrian Academy of Sciences, 6020 Innsbruck, Austria

<sup>3</sup>Institute for Theoretical Physics, University of Innsbruck, 6020 Innsbruck, Austria

<sup>4</sup>Institute of Atomic and Subatomic Physics, TU Wien, Stadionallee 2, 1020 Wien, Austria

(Received 21 January 2013; published 9 April 2013)

We propose and analyze a novel mechanism for long-range spin-spin interactions in diamond nanostructures. The interactions between electronic spins, associated with nitrogen-vacancy centers in diamond, are mediated by their coupling via strain to the vibrational mode of a diamond mechanical nanoresonator. This coupling results in phonon-mediated effective spin-spin interactions that can be used to generate squeezed states of a spin ensemble. We show that spin dephasing and relaxation can be largely suppressed, allowing for substantial spin squeezing under realistic experimental conditions. Our approach has implications for spin-ensemble magnetometry, as well as phonon-mediated quantum information processing with spin qubits.

DOI: 10.1103/PhysRevLett.110.156402

PACS numbers: 71.55.-i, 07.10.Cm, 42.50.Dv

Electronic spins associated with nitrogen-vacancy (NV) centers in diamond exhibit long coherence times and optical addressability, motivating extensive research on NV-based quantum information and sensing applications. Recent experiments have demonstrated coupling of NV electronic spins to nuclear spins [1,2], entanglement with photons [3], as well as single spin [4,5] and ensemble [6,7] magnetometry. An outstanding challenge is the realization of controlled interactions between several NV centers, required for quantum gates or to generate entangled spin states for quantum-enhanced sensing. One approach toward this goal is to couple NV centers to a resonant optical [8,9] or mechanical [10–12] mode; this is particularly appealing in light of rapid progress in the fabrication of diamond nanostructures with improved optical and mechanical properties [13–17].

In this Letter, we describe a new approach for effective spin-spin interactions between NV centers based on strain-induced coupling to a vibrational mode of a diamond resonator. We consider an ensemble of NV centers embedded in a single crystal diamond nanobeam, as depicted in Fig. 1(a). When the beam flexes, it strains the diamond lattice, which in turn couples directly to the spin triplet states in the NV electronic ground state [18,19]. For a thin beam of length  $L \sim 1 \mu\text{m}$ , this strain-induced spin-phonon coupling can allow for coherent effective spin-spin interactions mediated by virtual phonons. Based on these effective interactions, we explore the possibility of generating spin squeezing of an NV ensemble embedded in the nanobeam. We account for spin dephasing and mechanical dissipation and describe how spin echo techniques and mechanical driving can be used to suppress the dominant decoherence processes while preserving the coherent spin-spin interactions. Using these techniques we find

that significant spin squeezing can be achieved with realistic experimental parameters. Our results have implications for NV ensemble magnetometry and provide a new route toward controlled long-range spin-spin interactions.

*Model.*—The electronic ground state of the negatively charged NV center is a spin  $S = 1$  triplet with spin states labeled by  $|m_s = 0, \pm 1\rangle$  as shown in Fig. 1(b). In the presence of external electric and magnetic fields  $\vec{E}$  and  $\vec{B}$ , the Hamiltonian for a single NV is ( $\hbar = 1$ ) [19]

$$H_{\text{NV}} = (D_0 + d_{\parallel} E_z) S_z^2 + \mu_B g_s \vec{S} \cdot \vec{B} - d_{\perp} [E_x (S_x S_y + S_y S_x) + E_y (S_x^2 - S_y^2)], \quad (1)$$

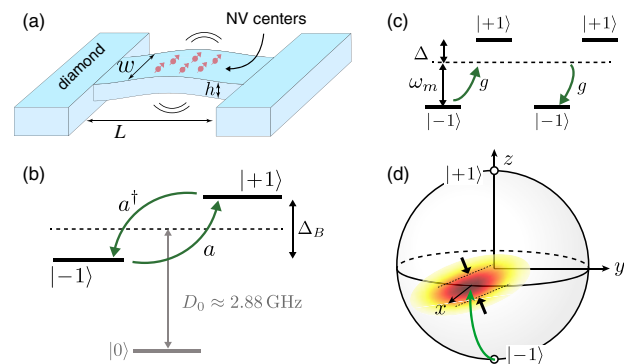


FIG. 1 (color online). (a) All-diamond doubly clamped mechanical resonator with an ensemble of embedded NV centers. (b) Spin triplet states of the NV electronic ground state. Local perpendicular strain induced by beam bending mixes the  $|\pm 1\rangle$  states. (c) A collection spins in the two-level subspace  $\{|+1\rangle, |-1\rangle\}$  is off-resonantly coupled to a common mechanical mode giving rise to effective spin-spin interactions. (d) Squeezing of the spin uncertainty distribution of an NV ensemble.

where  $D_0/2\pi \approx 2.88$  GHz is the zero field splitting,  $g_s \approx 2$ ,  $\mu_B$  is the Bohr magneton, and  $d_{\parallel}$  ( $d_{\perp}$ ) is the ground state electric dipole moment in the direction parallel (perpendicular) to the NV axis [20,21].

Motion of the diamond nanoresonator changes the local strain at the position of the NV center, which results in an effective, strain-induced electric field [19]. We are interested in the near-resonant coupling of a single resonant mode of the nanobeam to the  $|\pm 1\rangle$  transition of the NV, with Zeeman splitting  $\Delta_B = g_s \mu_B B_z / \hbar$ , as shown in Figs. 1(b) and 1(c). The perpendicular component of strain  $E_{\perp}$  mixes the  $|\pm 1\rangle$  states. For small beam displacements, the strain is linear in its position and we write  $E_{\perp} = E_0(a + a^\dagger)$ , where  $a$  is the destruction operator of the resonant mechanical mode of frequency  $\omega_m$ , and  $E_0$  is the perpendicular strain resulting from the zero point motion of the beam. We note that the parallel component of strain shifts both states  $|\pm 1\rangle$  relative to  $|0\rangle$  [22]; however, with near-resonant coupling  $\Delta = \Delta_B - \omega_m \ll D_0$  and preparation in the  $|\pm 1\rangle$  subspace, the state  $|0\rangle$  remains unpopulated and parallel strain plays no role in what follows. Within this two-level subspace, the interaction of each NV is  $H_i = g(\sigma_i^+ a + a^\dagger \sigma_i^-)$ , where  $\sigma_i^\pm = |\pm 1\rangle_i \langle \mp 1|$  is the Pauli operator of the  $i$ th NV center and  $g$  is the single phonon coupling strength. For many NV centers we introduce collective spin operators,  $J_z = \frac{1}{2} \sum_i |1\rangle_i \langle 1| - | -1\rangle_i \langle -1|$  and  $J_{\pm} = J_x \pm iJ_y = \sum_i \sigma_i^\pm$ , which satisfy the usual angular momentum commutation relations. The total system Hamiltonian can then be written as

$$H = \omega_m a^\dagger a + \Delta_B J_z + g(a^\dagger J_- + a J_+), \quad (2)$$

which describes a Tavis-Cummings type interaction between an ensemble of spins and a single mechanical mode [23]. In Eq. (2) we have assumed uniform coupling of each spin to the mechanical mode for simplicity; in general the coupling may be nonuniform. We also assume that the NVs are sufficiently far apart so that we may safely ignore direct dipole-dipole interactions between the spins. We discuss these points further below.

To estimate the coupling strength  $g$ , we calculate the strain for a given mechanical mode and use the experimentally obtained stress coupling of  $0.03$  Hz Pa $^{-1}$  in the NV ground state [24,25]. We take a doubly clamped diamond beam [see Fig. 1(a)] with dimensions  $L \gg w, h$  such that Euler-Bernoulli thin beam elasticity theory is valid [26]. For NV centers located near the surface of the beam we obtain [24]

$$\frac{g}{2\pi} \approx 180 \left( \frac{\hbar}{L^3 w \sqrt{\rho E}} \right)^{1/2} \text{ GHz}, \quad (3)$$

where  $\rho$  is the mass density and  $E$  is the Young's modulus of diamond. For a beam of dimensions  $(L, w, h) = (1, 0.1, 0.1)$   $\mu\text{m}$  we obtain a vibrational frequency  $\omega_m/2\pi \sim 1$  GHz and coupling  $g/2\pi \sim 1$  kHz. While

this is smaller than the strain coupling  $g_e/2\pi \approx 10$  MHz expected for electronic excited states of defect centers [27,28] or quantum dots [29], we benefit from the much longer spin coherence time  $T_2$  in the ground state. An important figure of merit is the single spin cooperativity  $\eta = (g^2 T_2) / (\gamma \bar{n}_{\text{th}})$ , where  $\gamma = \omega_m / Q$  is the mechanical damping rate and  $\bar{n}_{\text{th}} = (e^{\hbar\omega_m/k_B T} - 1)^{-1}$  is the equilibrium phonon occupation number at temperature  $T$ ; for example, the condition  $\eta > 1$  is sufficient to perform a quantum gate between two spins mediated by a thermal mechanical mode [10]. Assuming  $Q = 10^6$ ,  $T_2 = 10$  ms and  $T = 4$  K, we obtain a single spin cooperativity of  $\eta \sim 0.8$ . This can be further increased by reducing the dimensions of the nanobeam and operating at lower temperatures.

*Spin squeezing.*—In the dispersive regime,  $g \ll \Delta = \Delta_B - \omega_m$ , virtual excitations of the mechanical mode result in effective interactions between the otherwise decoupled spins. In this limit,  $H$  can be approximately diagonalized by the transformation  $e^R H e^{-R}$  with  $R = \frac{g}{\Delta} (a^\dagger J_- - a J_+)$ . To order  $(g/\Delta)^2$  this yields an effective Hamiltonian,

$$H_{\text{eff}} = \omega_m a^\dagger a + (\Delta_B + \lambda a^\dagger a) J_z + \frac{\lambda}{2} J_+ J_-, \quad (4)$$

where  $\lambda = 2g^2/\Delta$  is the phonon-mediated spin-spin coupling strength. Rewriting  $J_+ J_- = \mathbf{J}^2 - J_z^2 + J_z$ , and provided the total angular momentum  $J$  is conserved, we obtain a term  $\propto J_z^2$  corresponding to the one-axis twisting Hamiltonian [30].

To generate a spin squeezed state, we initialize the ensemble in a coherent spin state (CSS)  $|\psi_0\rangle$  along the  $x$  axis of the collective Bloch sphere. The CSS satisfies  $J_x |\psi_0\rangle = J |\psi_0\rangle$  and has equal transverse variances,  $\langle J_y^2 \rangle = \langle J_z^2 \rangle = J/2$ . This can be prepared using optical pumping and microwave spin manipulation applied to the ensemble [31]. The squeezing term  $\propto J_z^2$  describes a precession of the collective spin about the  $z$  axis at a rate proportional to  $J_z$ , resulting in a shearing of the uncertainty distribution and a reduced spin variance in one direction as shown in Fig. 1(d). This is quantified by the squeezing parameter [32,33],

$$\xi^2 = \frac{2J \langle \Delta J_{\min}^2 \rangle}{\langle J_x \rangle^2}, \quad (5)$$

where  $\langle \Delta J_{\min}^2 \rangle = \frac{1}{2} (V_+ - \sqrt{V_+^2 + V_{yz}^2})$  is the minimum spin uncertainty with  $V_{\pm} = \langle J_y^2 \pm J_z^2 \rangle$  and  $V_{yz} = \langle J_y J_z + J_z J_y \rangle / 2$ . The preparation of a spin squeezed state, characterized by  $\xi^2 < 1$ , has direct implications for NV ensemble magnetometry applications, since it would enable magnetic field sensing with a precision below the projection noise limit [32].

We now consider spin squeezing in the presence of realistic decoherence. In addition to the coherent dynamics

described by  $H_{\text{eff}}$ , we account for mechanical dissipation and spin dephasing using a master equation [24]

$$\dot{\rho} = -i \left[ -\frac{\lambda}{2} J_z^2 + (\Delta_B + \lambda a^\dagger a) J_z, \rho \right] + \frac{1}{2T_2} \sum_i \mathcal{D}[\sigma_z^i] \rho + \Gamma_\gamma (\bar{n}_{\text{th}} + 1) \mathcal{D}[J_-] + \Gamma_\gamma \bar{n}_{\text{th}} \mathcal{D}[J_+], \quad (6)$$

where  $\mathcal{D}[c]\rho = c\rho c^\dagger - \frac{1}{2}(c^\dagger c\rho + \rho c^\dagger c)$  and the single spin dephasing  $T_2^{-1}$  is assumed to be Markovian for simplicity (see below). Note that we absorbed a shift of  $\lambda/2$  into  $\Delta_B$ , and ignored single spin relaxation as  $T_1$  can be several minutes at low temperatures [34]. The second line describes collective spin relaxation induced by mechanical dissipation, with  $\Gamma_\gamma = \gamma g^2/\Delta^2$ . Finally, the phonon number  $n = a^\dagger a$  shifts the spin frequency, acting as an effective fluctuating magnetic field which leads to additional dephasing.

Let us for the moment ignore fluctuations of the phonon number  $n$ ; we address these in detail below. Starting from the CSS  $|\psi_0\rangle$ , we plot the squeezing parameter in Fig. 2(a) for an ensemble of  $N = 100$  spins and several values of  $\bar{n}_{\text{th}}$ , in the presence of dephasing  $T_2^{-1}$  and collective relaxation  $\Gamma_\gamma$ . Here we calculated  $\xi^2$  by solving Eq. (6) using an approximate numerical approach treating  $\Gamma_\gamma$  and  $T_2$  separately, and verified that the approximation agrees with exact results for small  $N$  [24]. To estimate the minimum squeezing, we linearize the equations of motion for the averages and variances of the collective spin operators [see dashed lines in Fig. 2(a)]. From these linearized equations, in the limits of interest,  $J \gg 1$ ,  $\bar{n}_{\text{th}} \gg 1$  and to leading order in both sources of decoherence, we obtain approximately

$$\xi^2 \simeq \frac{4\Gamma_\gamma \bar{n}_{\text{th}}}{J\lambda^2 t} + \frac{t}{T_2}. \quad (7)$$

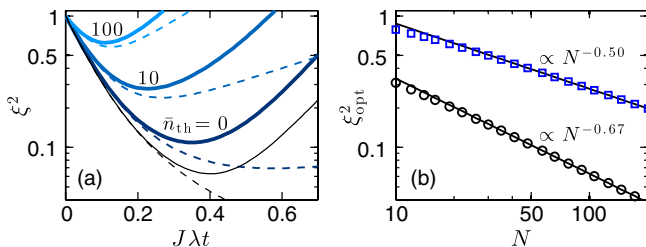


FIG. 2 (color online). (a) Spin squeezing parameter versus scaled precession time with  $N = 100$  spins. Thick blue (gray) lines show the calculated squeezing parameter for  $T_2 = 10$  ms and values of  $\bar{n}_{\text{th}}$  as shown. For each curve, we optimized the detuning  $\Delta$  to obtain the optimal squeezing. Dashed lines are calculated from the linearized equations for the spin operator averages. Thin black solid (dashed) line shows exact (linearized) unitary squeezing. (b) Optimal squeezing versus number of spins. Lower (upper) line shows power law fit for  $\bar{n}_{\text{th}} = 1$  (10) and  $T_2 = 1$  (0.01) s. The detuning  $\Delta$  is optimized for each point. Other parameters in both plots are  $\omega_m/2\pi = 1$  GHz,  $g/2\pi = 1$  kHz,  $Q = 10^6$ .

Optimizing  $t$  and the detuning  $\Delta$ , we obtain the optimal squeezing parameter,

$$\xi_{\text{opt}}^2 \simeq \frac{2}{\sqrt{J\eta}}, \quad (8)$$

at time  $t_{\text{opt}} = T_2/\sqrt{J\eta}$ , similar to results for atomic systems [35–37]. Note that for non-Markovian dephasing, the scaling is even more favorable [38]. In Fig. 2(b) we plot the scaling of the squeezing parameter with  $J$  for small but finite decoherence, and find agreement with Eq. (8). For comparison we also plot the unitary result in the absence of decoherence, scaling as  $\xi_{\text{opt}}^2 \sim J^{-2/3}$  and limited by the Bloch sphere curvature [30].

*Phonon number fluctuations.*—In Eq. (4) we see that the phonon number  $n = a^\dagger a$  couples to  $J_z$ , leading to additional dephasing due to thermal number fluctuations. On the other hand, this same coupling can also lead to additional spin squeezing from cavity feedback, by driving the mechanical mode [35–37]. In the following, we consider a twofold approach to mitigate thermal spin dephasing while preserving the optimal squeezing. First, we apply a sequence of global spin echo control pulses to suppress dephasing from low-frequency thermal fluctuations. This also extends the effective coherence time  $T_2$  of single NV spins [31]. Second, we consider driving the mechanical mode, and identify conditions when this results in a net improvement of the squeezing.

To simultaneously account for thermal dephasing, driven feedback squeezing, and spin control pulse sequences, we write the interaction term in Eq. (4) in the so-called toggling frame [39],

$$H_{\text{int}}(t) = \lambda J_z f(t) \delta n(t). \quad (9)$$

The function  $f(t)$  periodically inverts the sign of the interaction as shown in the inset of Fig. 3(a), describing the inversion of the collective spin  $J_z \rightarrow -J_z$  with each  $\pi$  pulse of the spin echo sequence. Phonon number fluctuations are described by  $\delta n(t) = n(t) - \bar{n}$ , where  $\bar{n}$  is the mean phonon number and we have omitted an average frequency shift proportional to  $\bar{n}$  in Eq. (9). The number fluctuation spectrum  $S_n(\omega) = \int dt e^{i\omega t} \langle \delta n(t) \delta n(0) \rangle$  is plotted in Fig. 3(a) for a driven oscillator coupled to a thermal bath [24].

We calculate the required spin moments within the Gaussian approximation for phonon number fluctuations, and obtain [24]

$$\langle J_+(t) \rangle = e^{-\chi} \langle e^{-i\mu(J_z - 1/2)} J_+(0) \rangle, \quad (10)$$

and similar results for  $\langle J_+^2(t) \rangle$  and  $\langle J_+(t) J_z(t) \rangle$ . In Eq. (10) the dephasing parameter  $\chi$  and effective squeezing via  $\mu$  are given by

$$\chi = \lambda^2 \int \frac{d\omega}{2\pi} \frac{F(\omega\tau)}{\omega^2} \bar{S}_n(\omega), \quad (11)$$

$$\mu = \lambda^2 \int \frac{d\omega}{2\pi} \frac{K(\omega\tau)}{\omega^2} A_n(\omega), \quad (12)$$

where  $\bar{S}_n(\omega) = [S_n(\omega) + S_n(-\omega)]/2$  and  $A_n(\omega) = [S_n(\omega) - S_n(-\omega)]/2$ . The filter function  $F(\omega\tau) = \frac{\omega^2}{2} |\int dt e^{i\omega t} f(t)|^2$  describes the effect of the spin echo pulse sequence with time  $\tau$  between  $\pi$  pulses [40–42]. The function  $K(\omega\tau)$  plays the analogous role for the effective squeezing described by  $\mu$ , and is related to  $F$  by a Kramers-Kronig relation [24]. We plot  $K$  and  $F$  for a sequence of  $M = 4$  pulses in Fig. 3(a).

*Discussion.*—We now consider the impact of thermal fluctuations on the achievable squeezing. The thermal noise spectrum  $S_n(\omega) = 2\gamma\bar{n}_{\text{th}}(\bar{n}_{\text{th}} + 1)/(\omega^2 + \gamma^2)$  is symmetric around  $\omega = 0$ . Without spin echo control pulses, this low-frequency noise results in nonexponential decay of the spin coherence,  $\chi_0(t) = \frac{1}{2}\lambda^2\bar{n}_{\text{th}}^2 t^2$  (with  $\bar{n}_{\text{th}} \gg 1$ ), familiar from single qubit decoherence [31,43]. The inhomogeneous thermal dephasing time is  $T_2^* \approx \sqrt{2}/\lambda\bar{n}_{\text{th}}$ , severely limiting the possibility of spin squeezing. In particular, at time  $t = t_{\text{opt}}$  we find that squeezing is prohibited when  $\bar{n}_{\text{th}} > \sqrt{J}$  [24]. However, one can overcome this low-frequency thermal noise using spin echo. By applying a sequence of  $M$  equally spaced global  $\pi$  pulses to the spins during precession of total time  $t$ , we obtain

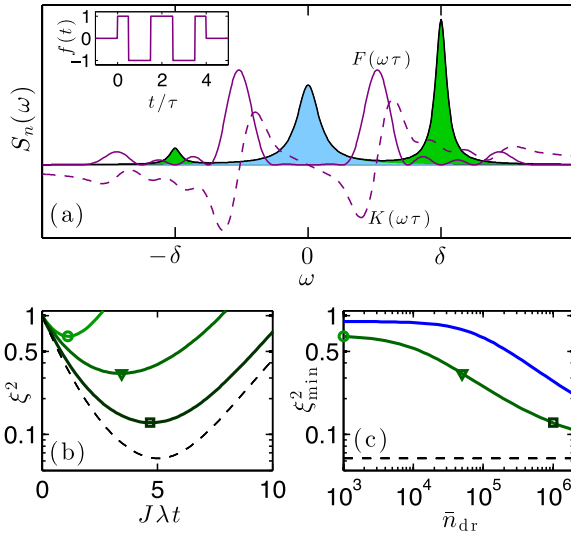


FIG. 3 (color online). (a) Number fluctuation spectrum of thermal driven oscillator. Center (blue filled) peak is purely thermal while side (green filled) peaks are due to detuned drive. Solid (dashed) purple line shows filter function  $F$  ( $K$ ) for  $M = 4$  pulses. Inset: corresponding function  $f(t)$  for  $M = 4$ . (b) Solid green curves show squeezing parameter versus precession time for  $\bar{n}_{\text{th}} = 10$  and  $\bar{n}_{\text{dr}} = 10^3, 5 \times 10^4, 10^6$  (top to bottom). Dashed black line shows unitary squeezing. (c) Minimum squeezing versus drive strength for  $\bar{n}_{\text{th}} = 50, 10$  (top to bottom). Symbols mark corresponding points with (b). Dashed black line shows unitary squeezing. Parameters in (b) and (c) are  $M = 4$ ,  $g/2\pi = 1$  kHz,  $T_2 = 10$  ms,  $N = 100$ ,  $\omega_m/2\pi = 1$  GHz,  $Q = 10^6$ .

$\chi_{\text{th}} \sim \lambda^2 \gamma \bar{n}_{\text{th}}^2 t^3 / M^2$ , suggesting that thermal dephasing can be made negligible relative to both  $\Gamma_\gamma$  and  $T_2^{-1}$ . For a sufficiently large number of pulses,  $M \gg \bar{n}_{\text{th}} \sqrt{\gamma T_2}$ , we recover the optimal squeezing in Eqs. (7) and (8).

Adding a mechanical drive can further enhance squeezing via feedback; however, it also increases phonon number fluctuations, contributing to additional dephasing. We consider a detuned external drive of frequency  $\omega_{\text{dr}} = \omega_m + \delta$ , leading to two additional peaks in  $S_n(\omega)$  at  $\omega = \pm\delta$ , as shown in Fig. 3(a). The area under the left [right] peak scales as  $\bar{n}_{\text{dr}}\bar{n}_{\text{th}}$  [ $\bar{n}_{\text{dr}}(\bar{n}_{\text{th}} + 1)$ ], where  $\bar{n}_{\text{dr}}$  is the mean phonon number due to the drive at zero temperature. The symmetric and antisymmetric parts of this noise contribute to dephasing and squeezing as described by Eqs. (11) and (12). Choosing the interval  $t/M = 2\pi/\delta$  between  $\pi$  pulses, we obtain additional dephasing  $\chi_{\text{dr}} \approx (\frac{\lambda}{\delta})^2 \bar{n}_{\text{dr}} \bar{n}_{\text{th}} \gamma t$  and effective squeezing with  $\mu \approx \frac{\lambda^2}{\delta} \bar{n}_{\text{dr}} t$ . In the limit  $\bar{n}_{\text{dr}} \gg \bar{n}_{\text{th}}$ , the effects of the drive dominate over  $\chi_{\text{th}}$  and  $\Gamma_\gamma$  and we recover the ideal scaling given in Eq. (8), even with a small number of echo pulses. This is shown in Figs. 3(b) and 3(c) where we see that the optimal squeezing improves with increasing  $\bar{n}_{\text{dr}}$  for a fixed number of pulses  $M = 4$ .

Finally, we discuss our assumption of uniform coupling strength  $g$  in Eq. (2). This is an important practical issue, as we expect the coupling to individual spins to be inhomogeneous in experiment due to the spatial variation of strain in the beam. Nonetheless, even with nonuniform coupling, we still obtain squeezing of a collective spin with a reduced effective total spin  $J_{\text{eff}} < J$ , provided  $J \gg 1$ . First, we note that inhomogeneous magnetic fields resulting in nonuniform detuning are compensated by spin echo. Second, for a distribution of coupling strengths  $g_i$ , the effective length of the collective spin is  $(\sum_i g_i)^2 / \sum_i g_i^2$  for the direct squeezing term, and  $(\sum_i g_i^2)^2 / \sum_i g_i^4$  for feedback squeezing with a mechanical drive. Similar conclusions were reached in atomic and nuclear systems [35–37,44]. In the case of direct squeezing, it is important that the sign of the  $g_i$ 's is the same to avoid cancellation; this is automatically achieved by using NV centers implanted on the top of the beam. For beam dimensions (1, 0.1, 0.1)  $\mu\text{m}$  analyzed above, we estimate that  $N \sim 200$  NV centers can be embedded without being perturbed by direct magnetic dipole-dipole interactions. A reduction of the effective spin length by factor  $\sim 2$  still leaves  $N_{\text{eff}} \sim 100$ , sufficient to observe spin squeezing.

*Conclusions.*—We have shown that direct spin-phonon coupling in diamond can be used to prepare spin squeezed states of an NV ensemble embedded in a nanoresonator, even in the presence of dephasing and mechanical dissipation. With further reductions in temperature, beam dimensions, and spin decoherence rates, the regime of large single spin cooperativity  $\eta \gg 1$  could be achieved. This would allow for coherent phonon-mediated interactions and quantum gates between two spins embedded in the

same resonator via  $H_{\text{int}} = \lambda(\sigma_1^+ \sigma_2^- + \text{H.c.})$ , and coupling over larger distances by phononic channels [27].

The authors gratefully acknowledge discussions with Shimon Kolkowitz and Quirin Unterreithmeier. This work was supported by NSF, CUA, DARPA, NSERC, HQOC, DOE, the Packard Foundation, the EU project AQUITE and the Austrian Science Fund (FWF) through SFB FOQUS and the START Grant No. Y 591-N16.

- 
- [1] F. Jelezko, T. Gaebel, I. Popa, M. Domhan, A. Gruber, and J. Wrachtrup, *Phys. Rev. Lett.* **93**, 130501 (2004).
- [2] L. Childress, M. V. G. Dutt, J. M. Taylor, A. S. Zibrov, F. Jelezko, J. Wrachtrup, P. R. Hemmer, and M. D. Lukin, *Science* **314**, 281 (2006).
- [3] E. Togan *et al.*, *Nature (London)* **466**, 730 (2010).
- [4] J. R. Maze *et al.*, *Nature (London)* **455**, 644 (2008).
- [5] G. Balasubramanian *et al.*, *Nature (London)* **455**, 648 (2008).
- [6] V. M. Acosta *et al.*, *Phys. Rev. B* **80**, 115202 (2009).
- [7] L. M. Pham *et al.*, *New J. Phys.* **13**, 045021 (2011).
- [8] D. Englund, B. Shields, K. Rivoire, F. Hatami, J. Vuckovic, H. Park, and M. D. Lukin, *Nano Lett.* **10**, 3922 (2010).
- [9] A. Faraon, P. E. Barclay, C. Santori, K.-M. C. Fu, and R. G. Beausoleil, *Nat. Photonics* **5**, 301 (2011).
- [10] P. Rabl, S. J. Kolkowitz, F. H. L. Koppens, J. G. E. Harris, P. Zoller, and M. D. Lukin, *Nat. Phys.* **6**, 602 (2010).
- [11] O. Arcizet, V. Jacques, A. Siria, P. Poncharal, P. Vincent, and S. Seidelin, *Nat. Phys.* **7**, 879 (2011).
- [12] S. Kolkowitz, A. C. B. Jayich, Q. P. Unterreithmeier, S. D. Bennett, P. Rabl, J. G. E. Harris, and M. D. Lukin, *Science* **335**, 1603 (2012).
- [13] B. J. M. Hausmann, J. T. Choy, T. M. Babinec, B. J. Shields, I. Bulu, M. D. Lukin, and M. Lončar, *Phys. Status Solidi A* **209**, 1619 (2012).
- [14] P. Ouartchaiyapong, L. M. A. Pascal, B. A. Myers, P. Lauria, and A. C. B. Jayich, *Appl. Phys. Lett.* **101**, 163505 (2012).
- [15] M. K. Zalalutdinov, M. P. Ray, D. M. Photiadis, J. T. Robinson, J. W. Baldwin, J. E. Butler, T. I. Feygelson, B. B. Pate, and B. H. Houston, *Nano Lett.* **11**, 4304 (2011).
- [16] M. J. Burek, N. P. de Leon, B. J. Shields, B. J. M. Hausmann, Y. Chu, Q. Quan, A. S. Zibrov, H. Park, M. D. Lukin, and M. Lončar, *Nano Lett.* **12**, 6084 (2012).
- [17] Y. Tao, J. M. Boss, B. A. Moores, and C. L. Degen, *arXiv:1212.1347*.
- [18] J. R. Maze, A. Gali, E. Togan, Y. Chu, A. Trifonov, E. Kaxiras, and M. D. Lukin, *New J. Phys.* **13**, 025025 (2011).
- [19] M. Doherty, F. Dolde, H. Fedder, F. Jelezko, J. Wrachtrup, N. B. Manson, and L. C. L. Hollenberg, *Phys. Rev. B* **85**, 205203 (2012).
- [20] E. Vanoort and M. Glasbeek, *Chem. Phys. Lett.* **168**, 529 (1990).
- [21] F. Dolde *et al.*, *Nat. Phys.* **7**, 459 (2011).
- [22] V. M. Acosta, E. Bauch, M. P. Ledbetter, A. Waxman, L.-S. Bouchard, and D. Budker, *Phys. Rev. Lett.* **104**, 070801 (2010).
- [23] M. Tavis and F. W. Cummings, *Phys. Rev.* **170**, 379 (1968).
- [24] See Supplemental Material at <http://link.aps.org/supplemental/10.1103/PhysRevLett.110.156402> for details on coupling strength, decoherence, and phonon number fluctuations.
- [25] E. Togan, Y. Chu, A. Imamoglu, and M. D. Lukin, *Nature (London)* **478**, 497 (2011).
- [26] L. D. Landau and E. M. Lifshitz, *Theory of Elasticity* (Butterworth-Heinemann, Oxford, 1986).
- [27] S. J. M. Habraken, K. Stannigel, M. D. Lukin, P. Zoller, and P. Rabl, *New J. Phys.* **14**, 115004 (2012).
- [28] O. O. Soykal, R. Ruskov, and C. Tahan, *Phys. Rev. Lett.* **107**, 235502 (2011).
- [29] I. Wilson-Rae, P. Zoller, and A. Imamoglu, *Phys. Rev. Lett.* **92**, 075507 (2004).
- [30] M. Kitagawa and M. Ueda, *Phys. Rev. A* **47**, 5138 (1993).
- [31] J. M. Taylor, P. Cappellaro, L. Childress, L. Jiang, D. Budker, P. R. Hemmer, A. Yacoby, R. Walsworth, and M. D. Lukin, *Nat. Phys.* **4**, 810 (2008).
- [32] D. J. Wineland, J. J. Bollinger, W. M. Itano, F. L. Moore, and D. J. Heinzen, *Phys. Rev. A* **46**, R6797 (1992).
- [33] J. Ma, X. g. Wang, C. P. Sun, and F. Nori, *Phys. Rep.* **509**, 89 (2011).
- [34] A. Jarmola, V. M. Acosta, K. Jensen, S. Chemerisov, and D. Budker, *Phys. Rev. Lett.* **108**, 197601 (2012).
- [35] M. H. Schleier-Smith, I. D. Leroux, and V. Vuletic, *Phys. Rev. A* **81**, 021804(R) (2010).
- [36] I. D. Leroux, M. H. Schleier-Smith, and V. Vuletic, *Phys. Rev. Lett.* **104**, 073602 (2010).
- [37] I. D. Leroux, M. H. Schleier-Smith, H. Zhang, and V. Vuletic, *Phys. Rev. A* **85**, 013803 (2012).
- [38] D. Marcos, M. Wubs, J. M. Taylor, R. Aguado, M. D. Lukin, and A. S. Sørensen, *Phys. Rev. Lett.* **105**, 210501 (2010).
- [39] U. Haeblerlen and J. Waugh, *Phys. Rev.* **175**, 453 (1968).
- [40] L. Cywiński, R. M. Lutchyn, C. P. Nave, and S. DasSarma, *Phys. Rev. B* **77**, 174509 (2008).
- [41] J. M. Martinis, S. Nam, J. Aumentado, K. M. Lang, and C. Urbina, *Phys. Rev. B* **67**, 094510 (2003).
- [42] G. S. Uhrig, *Phys. Rev. Lett.* **98**, 100504 (2007).
- [43] R. de Sousa, *Top. Appl. Phys.* **115**, 183 (2009).
- [44] M. Rudner, L. M. K. Vandersypen, V. Vuletic, and L. S. Levitov, *Phys. Rev. Lett.* **107**, 206806 (2011).